AIAA 80-0390R

Outer Zone Energetic Electron Spectral Measurements

J. B. Reagan,* R. W. Nightingale,† E. E. Gaines,‡ and W. L. Imhof§
Lockheed Palo Alto Research Laboratory, Palo Alto, Calif.
and
E. G. Stassinopoulos¶
National Space Science Data Center, Greenbelt, Md.

Detailed spectral measurements of energetic electrons between 47 and 5100 keV have been made with the SC-3 experiment aboard the P78-2 (SCATHA) spacecraft. During the period Jan. 29-Feb. 2, 1979 the spacecraft was in a highly elliptical orbit. Measurements of the outer radiation belt electrons from 3.5 to 8.0 Earth radii were made near the geomagnetic equator. Spin-averaged electron spectra in 12-24 energy channels have been obtained. The magnetic activity at the time of the measurements was low, but a modest magnetic storm ($D_{st} = -79$ γ) had occurred ~10 days earlier. Comparisons of the measured radial profiles and electron spectra with the NASA AE-4 and AEI-7 HI/LO radiation models have been made. Under these conditions the measured data are in better agreement with the AE-4 model than with the AEI-7 HI model, although the present data are more intense above 4 MeV than the AE-4 model. The impact of the measured spectrum on the dose profile encountered by a synchronous orbit satellite has been examined. For thin aluminum shields (<0.45 cm) the dose received is comparable using either the AE-4 or AEI-7 models or the measured spectra. For thicker shields the bremsstrahlung dose dominates over the direct electron effects.

Introduction

THE USAF Space Test Program P78-2 spacecraft, known as the Spacecraft-Charging-At-High-Altitudes (SCATHA) mission, was launched on Jan. 30, 1979 into a highly elliptical transfer orbit having an apogee of 43,183 km, a perigee of 176 km, and an inclination of 27.3 deg. The spacecraft remained in this orbit until Feb. 2, 1979, at which time an adjustment was initiated to provide the final, near-synchronous orbit at 7.9 deg inclination with apogee at 43,192 km, perigee at 27,517 km, and period of 23.597 hours. Included in the P78-2 payload complement is a high-energy particle spectrometer known as SC-3. This spectrometer, which is described in detail in the mission description report,[1] measures energetic electrons between 47 keV and 5100 keV, protons between 1 and 200 MeV, and alpha particles between 6 and 60 MeV in several selectable modes of operation.

The P78-2 transfer orbit provided a unique opportunity to study the entire outer radiation belt region from 3.5 to 8.0 Earth radii distance near the geomagnetic equator during this solar maximum epoch. In particular, the fine resolution and extended energy range of the spectrometer provides the opportunity to define the spectrum of the energetic electrons for comparison with existing radiation belt models. These data are of significant interest to spacecraft designers and mission planners in that the electrons in the MeV energy range contribute the dominant radiation dose to satellites operating in this region of space.[2] Long-duration synchronous satellite missions are significantly constrained by the shielding that must be included to mitigate the degradation and damaging effects of these electrons and their associated bremsstrahlung. The optimum shielding design of such spacecraft is critically linked to the accuracy to which the very energetic electron fluence is known over the mission lifetime. Because of the short duration of the transfer orbit, the present data cannot provide the long-term averages required for mission planning but can provide a complete radial profile of spectral shape and flux for comparison with the radiation models at this time in the solar cycle. In the final orbit the opportunity exists to analyze an almost continuous data base in the year 1979, and hopefully thereafter, between 5.2 and 8.0 Earth radii, which encompasses the synchronous orbit. When analyzed, these data should provide the long-term averages necessary for high-altitude spacecraft mission planning. In this first publication of the SC-3 results we confine our analysis to the transfer orbit period.

Experiment Description and Operations

In the transfer orbit the SC-3 experiment was operated during real-time acquisition intervals only since the satellite tape recorder was not yet operational. The satellite was also spinning at a high rate of 1.04 rev/s as compared to the final orbit spin rate of 1.0 rev/min. The spin axis of the satellite is maintained perpendicular to the sun-Earth line such that in a single spin the SC-3 instrument scans through a complete pitch angle distribution. Since the sampling rate of the SC-3 spectra is twice per second, integration over one-half of the spin period or 180 deg in pitch angle resulted, while in the final orbit pitch angle measurements every 3 deg are being routinely obtained. Because of the limited angular resolution and the lack of magnetometer data, only spin-averaged electron data are reported in this paper. The SC-3 experiment was operated primarily in the electron modes during this period although some limited proton data were acquired. When the spectrometer is powered on, automatic operation is achieved in a hardwired mode, called BACKUP, that measured electrons between 240 and 5078 keV in 12 quasilogarithmic energy channels. The spectrometer can also be operated from an internal memory which determines the sensor to be analyzed, the logic configuration between the several sensors in the solid-state particle telescope, and the energy range to be analyzed. The telescope, shown in cross section in Fig. 1, consists of a 200-μ-thick surface-barrier silicon detector, D, that is used to analyze electrons in the 47-300 keV energy range. Following this detector is a stack of five 2-mm-thick surface-barrier silicon detectors connected in parallel for a total stopping range of 1 cm. This detector stack, E, is used to analyze electrons between 300 and 5100

Presented as Paper 80-0390 at the AIAA 18th Aerospace Sciences Meeting, Pasadena, Calif., Jan. 14-16, 1980; submitted Feb. 7, 1980; revision received Aug. 26, 1980. Copyright © American Institute of Aeronautics and Astronautics, Inc., 1980. All rights reserved.

*Manager, Space Sciences Laboratory.
†Senior Scientist, Space Sciences Laboratory.
‡Research Scientist, Space Sciences Laboratory.
§Technical Development Leader, Space Sciences Laboratory.
¶Astrophysicist.

Table 1 Characteristics of the SC-3 electron spectrometer in the transfer orbit

	BACKUP mode			ELEC 1 mode			ELEC 2 mode		
Channel	Energy, MeV	ΔE, MeV	$(G\epsilon\Delta E)^{-1}$, $(cm^2\text{-sr-MeV})^{-1}$	Energy, MeV	ΔE, MeV	$(G\epsilon\Delta E)^{-1}$, $(cm^2\text{-sr-MeV})^{-1}$	Energy, MeV	ΔE, MeV	$(G\epsilon\Delta E)^{-1}$, $(cm^2\text{-sr-MeV})^{-1}$
1	0.24-0.36	.12	9.76E3	.047-.066	.019	1.99E4	0.26-0.63	.37	1.74E3
2	0.36-0.49	.13	5.09E3	.066-.087	.021	1.87E4	0.63-1.03	.40	1.05E3
3	0.49-0.62	.13	3.79E3	.087-.108	.021	1.83E4	1.03-1.42	.39	1.08E3
4	0.62-0.75	.13	3.12E3	.108-.129	.021	1.83E4	1.42-1.81	.39	1.14E3
5	0.75-0.89	.14	3.04E3	.129-.150	.021	1.83E4	1.81-2.21	.40	1.22E3
6	0.89-1.02	.13	3.06E3	.150-.171	.021	1.83E4	2.21-2.60	.39	1.26E3
7	1.02-1.70	.68	6.34E2	.171-.192	.021	1.86E4	2.60-3.00	.40	1.38E3
8	1.70-2.37	.67	7.13E2	.192-.214	.022	1.79E4	3.00-3.39	.39	1.48E3
9	2.37-3.05	.68	8.26E2	.214-.235	.021	1.95E4	3.39-3.79	.40	1.80E3
10	3.05-3.73	.68	1.06E3	.235-.256	.021	2.22E4	3.97-4.18	.39	2.14E3
11	3.73-4.40	.67	1.37E3	.256-.278	.022	2.55E4	4.18-4.58	.40	3.25E3
12	4.40-5.08	.68	2.08E3	.278-.299	.021	3.29E4	4.58-4.97	.39	3.68E3

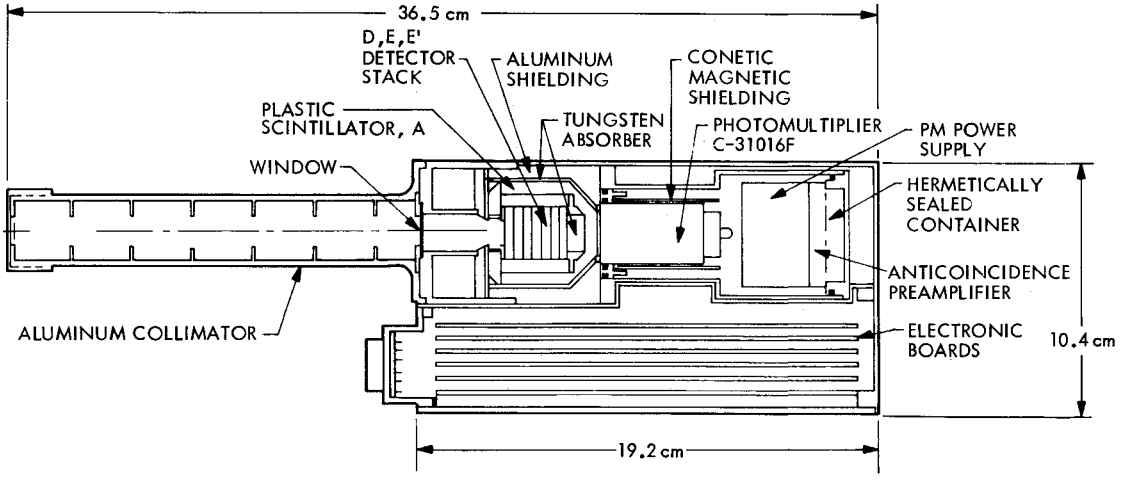

Fig. 1 Cross-section of the SC-3 spectrometer.

keV. Following the thick stack is a 1-mm-thick detector, E′, that is used as an active anticoincidence collimator operating on high-energy particles that penetrate the detector stack. The entire silicon detector assembly is surrounded by a plastic scintillator anticoincidence guard, A, that is effective in eliminating very energetic charged particles that penetrate the outer walls of aluminum and tungsten.

The aluminum shielding is sufficiently thick to stop electrons effectively with energy up to 5 MeV. Bremsstrahlung photons with energy <150 keV created in the low-atomic-number aluminum are effectively attenuated by the tungsten shield located inside the aluminum and around the scintillator. Bremsstrahlung photons $\gtrsim 150$ keV are not effectively attenuated in the tungsten nor detected in the plastic scintillator. A fraction of these photons can interact in the E detector. Laboratory measurements using intense Sr-Y-90 sources at normal incidence to the shielding showed that the resulting bremsstrahlung count rate was only 3.4×10^{-4}, 5.1×10^{-4}, and 6.4×10^{-5} of the electron count rate at energies of 250, 500, and 100 keV, respectively. The bremsstrahlung detection efficiency in the D detector was determined to be completely insignificant because of the small volume of this sensor.

The sensors were energy-calibrated prior to launch with several radioactive sources, including weak Americium-241 sources that were included in the flight instrument. Special high-energy resolution analyses of these sources on-orbit on a daily basis have shown no shift in the laboratory calibrations and a stability of better than 1% over the first several months of operation. Electron detection efficiencies have been calculated as a function of energy using a Fokker-Planck analytic approach in which the electrons are tracked as they diffuse through the silicon. This approach produced results very comparable to the Monte Carlo approach of Berger et al.[3] which are in excellent agreement with experimental data. Detection efficiences over the energy ranges analyzed were typically much greater than 0.5. Geometric factors were calculated using the geometry of the collimator and sensors with consideration being given to large angle scattering in certain of the telescope elements. The directional geometric factor in the D sensor is 3.0×10^{-3} cm^2-sr while the E sensor stack varied from 2.92×10^{-3} cm^2-sr at the front to 2.37×10^{-3} cm^2-sr at the rear. A very detailed determination of the angular response function of the narrow collimation system was performed in a vacuum chamber prior to flight using an intense Sr-Y-90 electron source located at a large distance from the spectrometer which was situated on a precision rotation table. The long collimator (20 cm) containing 10 baffles that defined the 3 deg FWHM response of the spectrometer was experimentally shown to agree with the calculated geometrical response function.

At times in the transfer orbit the spectrometer was also operated from the internal memory in two time sequenced modes. In the first mode (ELEC 1), electron fluxes detected in the D sensor from 47 to 300 keV were analyzed for 8 s with the 12-channel pulse height analyzer in the spectrometer operating in a linear manner. In the following 8 s, electrons detected in the E detector between 263 and 4970 keV were analyzed in the ELEC 2 mode by the same analyzer. This pattern was continuously repeated. In all of the modes of operation the single counting rates from the D, E, E′, and A sensors are obtained such that dead time and chance coin-

cidence rates can be calculated. The essential characteristics of the SC-3 spectrometer are summarized in Table 1.

Data

The P78-2 transfer orbit was transformed into B,L space as a means of organizing the electron fluxes. The parameter L defines a dipole-like magnetic shell along which the electrons execute their bounce and drift motion around the Earth and B is the magnetic field intensity that specifies a position along this shell between the equator and the particle mirror points. At the magnetic equator the value of L is expressed in multiples of Earth radii distance to that shell. Thus, the transfer orbit covered a range of $3.5<L<8.0$. The Institute of Geological Sciences/1975 (IGS/75) internal source model of Barraclough et al.[4] updated for the epoch 1979.1 was used to generate the magnetic field. A comparison of this model with a total field model including the above internal field model and the Olson and Pfitzer[5] external field was also made. Differences of $\pm 0.1L$ to $\pm 0.15L$ were observed between the models over the L range and local times covered in the transfer orbit. The sign of the difference was related to B, the indicator of the position along the magnetic field line. Since these differences were, in general, within the sorting bin size to be used for the particle data, only the internal field model was used in the final analysis. The minimum value, B_0, along a magnetic shell was determined from a field line tracing program. In this study the maximum value of B/B_0 used at any L was 2.2 and hence the data set is truly representative of the geomagnetic equator region. The magnetic shell parameter, L, in Earth radii, was determined using the formalism of McIlwain.[6] Omnidirectional differential electron spectra were generated at 2-min intervals along the orbital path using the AE-4[7] and the interim AEI-7 HI and LO[8] radiation belt models applicable to this region of space. These intervals were sufficiently fine such that comparisons of the model spectra with the measured data in narrow L intervals could be directly made.

The SC-3 spin-averaged data were then sorted by magnetic shell, L, into intervals of $\pm 0.1L$ centered on each $0.5L$ between 3.5 and 8.0 corresponding to the available data over the three-day period. Electron fluxes were obtained by dividing the spin-averaged counting rates in each channel by the energy width of the channel and the spin-averaged geometric factors. The latter were obtained by integrating the directional geometric factors over 4π solid angle. In some L intervals the instrument was operated in both the BACKUP and ELEC 1/ELEC 2 modes and additional energy channels were therefore obtained. In some intervals only the BACKUP data were available. Excellent counting statistics were obtained in all modes and intervals of operation except at the highest energy channels on the highest L-shells. A background contribution from the Americium-241 calibration source was present in the highest three energy channels of the E detector, i.e. above 3.8 MeV. On the magnetic shells $L<6$ this was a small effect due to the high fluxes encountered, and since the characteristics of the source were well known from daily on-orbit calibrations, this background could be subtracted. For $L>6$ due to the lower fluxes at the higher energies the calibration source background was more significant and dominated the statistical accuracy of the results above 3.8 MeV. In the range $3.5<L<6.0$ a significant bremsstrahlung background was also identified in the lowest channel of the E detector in the BACKUP and ELEC 2 modes. This was corrected by recognizing the contiguous energy relationship between the last channel of the ELEC 1 mode and the first channel of the ELEC 2 mode and the fact that the D detector had no significant bremsstrahlung background in laboratory tests. The laboratory measured bremsstrahlung spectrum shape for SR-Y-90 electrons which simulate the outer belt electrons was normalized in intensity to the first channel of the BACKUP mode such that the difference agreed with the last channel of the ELEC 1 mode. With this technique the bremsstrahlung background corrections to the remaining channels of the ELEC 2 mode were relatively small and totally insignificant above ~600 keV in energy. Dead time corrections never exceeded 20%.

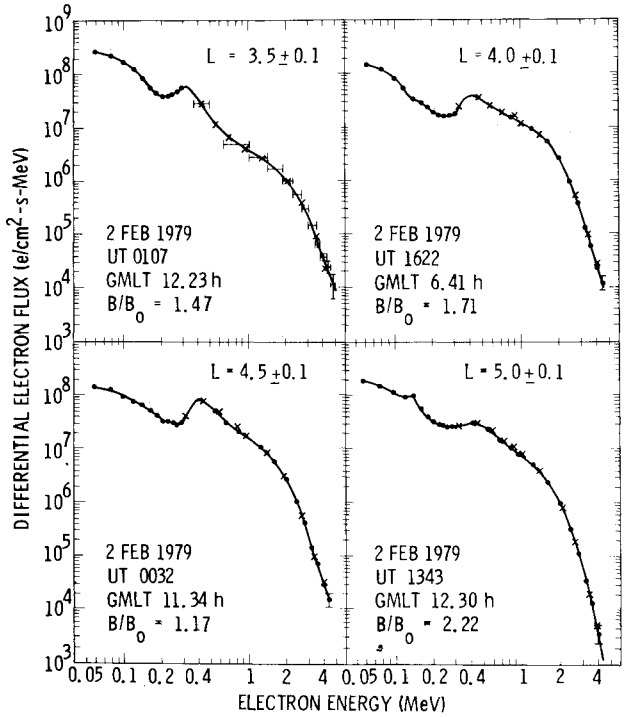

Fig. 2 Measured spin-averaged differential electron spectra for the L shells 3.5, 4.0, 4.5 and 5.0.

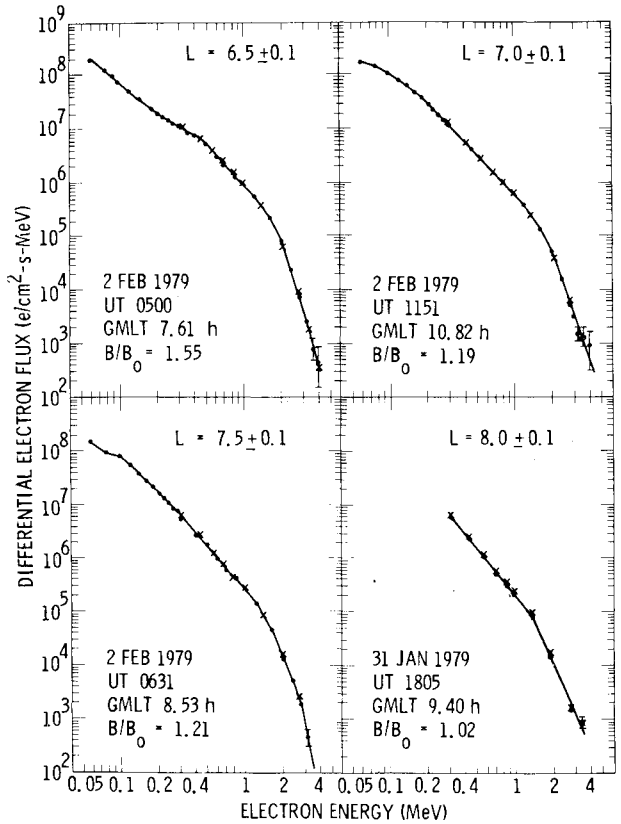

Fig. 3 Measured spin-averaged differential electron spectra for the L shells 6.5, 7.0, 7.5 and 8.0.

Examples of the spectral data obtained are shown in Figs. 2 and 3. For the $3.5<L<5.0$ range shown in Fig. 2 complex

spectral shapes over the entire energy range are observed. The statistical error in each energy channel is less than the width of the data point except where the actual error bars are shown. The complex spectral shapes are therefore statistically meaningful. Note that the spectra are representative of the geomagnetic equator in each case since the maximum B/B_0 is 2.2. To put these data in perspective one must examine earlier reports[2,9,10] on the spectral evolution of the electron fluxes in this region of space following a magnetic storm. At the time of a storm the flux levels increase at all energies; a smooth spectral shape is observed which then proceeeds to decay perhaps because the limiting fluxes on a given field line have been exceeded. The spectra following a storm show considerable structure for some 30 days or until a new storm occurs. When compared to the smooth injection spectrum, deep depressions are observed to form during this post storm period in the 200-1000 keV energy range.[2,9,10] The depressions may result from the precipitation of the electrons into the atmosphere over a several day period due to wave-particle interactions. The P78-2 data shown in Fig. 2 were taken 10 days after a modest storm had occurred in the magnetosphere on Jan. 23-24, 1979 with a maximum $D_{st} = -79\ \gamma$. The next previous storm occurred on Jan. 7, 1979 with a maximum $D_{st} = -94\ \gamma$. The parameter D_{st} is a measure of the departure, i.e. disturbance, of the horizontal component of the Earth's magnetic field from a normal dipole-like configuration as a result of increased solar-wind pressure. D_{st} has the units of γ ($1\ \gamma = 10^{-5}$ G) and typical magnetic storms produce a 50-100 γ negative deflection in the field during the main phase. The data of West et al.[9] clearly show that magnetic storms having D_{st} values of -79 to $-95\ \gamma$ cause significant changes in the trapped electron population in the equatorial region. The depression in the spectra on Feb. 2, 1979 shown in Fig. 2 between ~100 and 400 keV probably reflects the precipitation of these electrons into the atmosphere sometime following the storm on Jan. 24. The depressions are most pronounced between $3.5 \leq L \leq 4.5$ and exhibit remarkable similarity to the previously reported spectra for other post-storm periods,[2,9,10] albeit at slightly lower energies and not as deep perhaps because of the modest nature of the preceding storm. In the absence of these depressions a power-law spectrum would fit between 50 and 1500 keV but a completely different spectral shape exists above 1500 keV, as also previously recognized.[2] With such complex spectral evolution following a storm the task of developing a radiation model that encompasses and averages these temporal effects is indeed difficult and requires almost a continuous data base in time along with pitch angle distribution knowledge and extended energy range coverage.

Figure 3 illustrates the contrast in spectral shapes observed on the higher L-shells at this time. The spectra for $6.5 \leq L \leq 8.0$ are remarkably smooth and devoid of depressions but as in the case of the lower L-shells reflect at least a two component source/loss mechanism in that the spectra >1500 keV are quite different than below this energy. Also note the relative independence with L and constancy of the flux near 50 keV. The integral fluxes >50 keV are near the Kennel-Petschek[11] trapping limit.

Comparisons with Models

The measured spectra have been compared with the existing radiation models for this region of space in Fig. 4. The P78-2 spectra for the L-shells 4.0, 5.0, and 6.5, the latter being the representative of the Earth-synchronous orbit, are plotted on a semi-log scale to illustrate the truly exponential shape of the spectra >1.5 MeV. Also plotted are the AE-4 model[7] spectra and the new interim model AEI-7[8] with the LO and HI

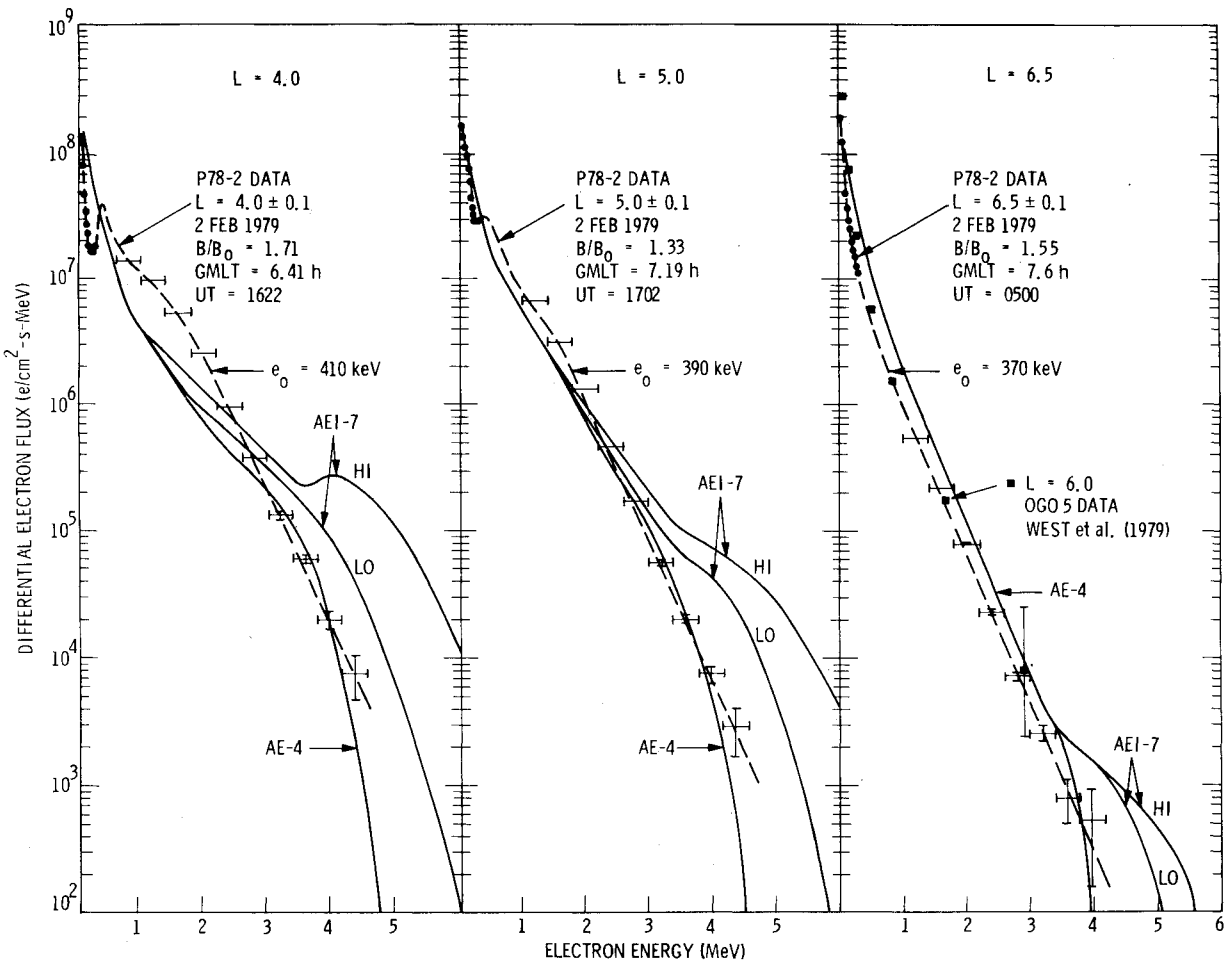

Fig. 4 Comparisons of the measured P78-2 spectra near the equator with the AE-4 and AEI-7 radiation models and with the data of West et al.[9]

versions reflecting the analysis of the OV1-19 data set by Chan et al.[8] and Vampola et al.,[10] respectively. The model differential spectra were derived for the same B,L position in the P78-2 transfer orbit as the measured spectra and hence any B/B_0 dependence, even though small, has been removed.

The spectral depressions observed at $L=4.0$ are not included in the models and hence the measurements are a factor of 4-5 lower than the models at energies around a few hundred keV. Between 500 keV and 3 MeV the measurements are more intense than the model values by a maximum factor of 4. Between 3 and 4 MeV the data and the AE-4 model are in good agreement, but above 4 MeV the AE-4 model spectrum falls abruptly while the measurements show that the spectrum continues in an exponential manner to at least 4.5 MeV. At 4.5 MeV the measured data are approximately a factor of 5 higher than the AE-4 model. Since these high-energy electrons are very significant in determining the radiation dose behind thick shields, this difference is important. Also note however that the measured data >3 MeV are significantly below either the AEI-7 LO or HI models. The AEI-7 HI model flux at 4.5 MeV is a factor of 17 higher than the measured flux and hence is not a good representation at this time. The AEI-7 LO model flux at 4.5 MeV is a factor of 5 higher than the measured flux and hence would provide a conservative modeling of the actual flux at this time.

At $L=5.0$, where the spectral depression is less pronounced, the agreement between the measured data and the AE-4 model is quite good up to 4 MeV, but again the model spectrum falls too abruptly above this energy. At 4.5 MeV the AE-4 model is a factor of 15 below the best-fit to the measured flux, but the AEI-7 LO and HI model flux are factors of 10 and 25 higher than the data, respectively. Thus, at these higher energies the AE-4 model underestimates the dose received and the AEI-7 model overestimates the dose, at least for the time of the measured data.

At $L=6.5$, which is representative of the Earth-synchronous orbit when longitude variations are considered, the measured data have the same spectral shape but are approximately a factor of 2 lower than the model data up to ~3 MeV. This difference may not be significant in that the P78-2 data were obtained at a geomagnetic local time of 7.6 h and previous satellite data have shown almost an order of magnitude diurnal variation in the very energetic electron fluxes at these altitudes. Above 3.5 MeV the AE-4 spectrum falls too abruptly while the AEI-7 LO and HI value is a factor of 3 higher. Once again, the AEI-7 LO spectrum would provide a conservative modeling for dose considerations. The AEI-7 HI model is too intense above 4 MeV and hence would give an overestimate of the dose. Also shown in Fig. 4 for $L=6.5$ are the recent data of West et al.[9] for $L=6.0$ which those authors feel is representative of the synchronous orbit at all but very disturbed periods. The present data are in excellent agreement with the West et al. data up to the 2.83 MeV limit of the latter. The bar on the West et al. data reflects the range over which the flux can vary during non-highly-disturbed periods.

Two remarkable features of the P78-2 measured energetic electron spectra >2.0 MeV are the truly exponential form and the L-independence of the slope, e_0, over the L range 4.0-6.5. As shown in Fig. 3 the e_0 values at $L=4.0$, 5.0, and 6.5 are 410, 390, and 370 keV, respectively. Radial diffusion is apparently not dominant at this time or a more significant hardening of the spectrum with decreasing L value would be observed. The source, acceleration, and loss processes for these very energetic electrons are obviously not well understood.

The relatively good agreement between the measured P78-2 data and the AE-4 model fluxes up to an energy of 4 MeV is illustrated in the radial profile comparison shown in Fig. 5. The largest difference between the measured flux and the model over this energy range is approximately a factor of 2.5. At certain energies, for example 3 MeV, the agreement is excellent. At 4.0 MeV the measured fluxes are uniformly higher than the model by less than a factor of 2 but above this energy the differences would become more significant, as indicated earlier. At the higher L-shells the very good agreement may be fortuitous in that the measured data are for a given local time while the model averages over the significant local time variations. A more meaningful comparison can be performed when the full SC-3 final orbit data set are analyzed.

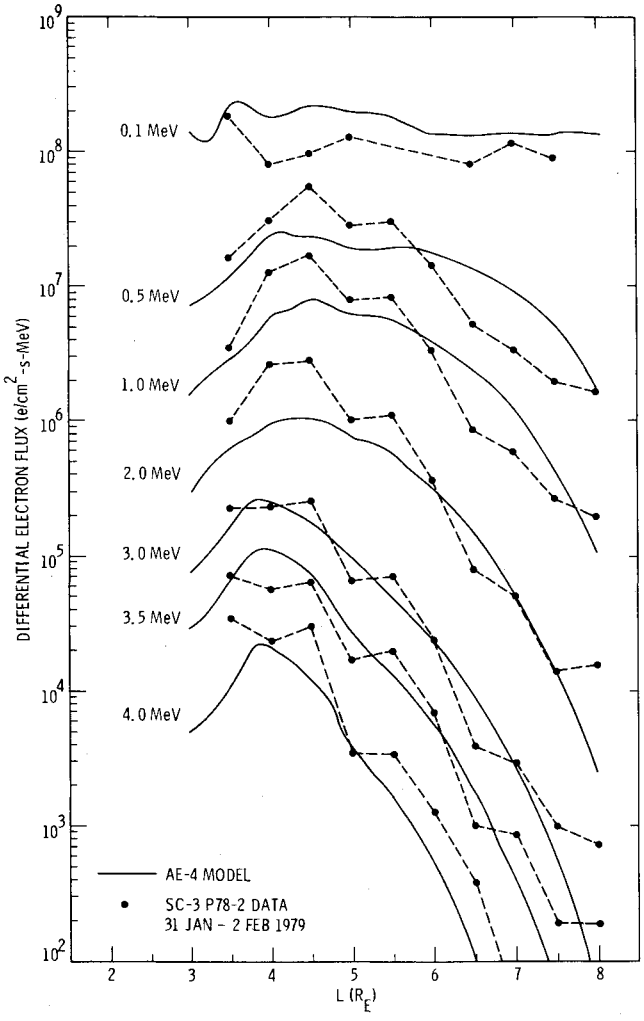

Fig. 5 Comparisons of the measured radial profile of the spin-averaged differential electron flux with the AE-4 model.

Dose Effects

The radiation dose impact associated with the various spectra shown in Fig. 4 for the geosynchronous orbit ($L=6.5$) has been determined. In performing these calculations the P78-2 spectrum shown in Fig. 4 has been normalized in intensity to the AE-4 spectra near 2 MeV on the rationale that the latter represents a better long-term average at that energy than the temporally limited P78-2 data set. Differences in the dose impact of the AE-4, AEI-7, and P78-2 spectra will therefore arise principally from the electrons $\gtrsim$ 3.5 MeV where the various spectra diverge. The dose calculations were performed as a function of spherical aluminum shield thickness. The computer program used to generate the dose solves analytically the Fokker-Planck diffusion equation to obtain the energy deposited by electrons of a specified input spectrum and angular distribution as they migrate through the aluminum. Scattering of the electrons throughout the shield is tracked. The dose program is an adaption of the AURORA program developed by Walt et al.[12] The dose associated with

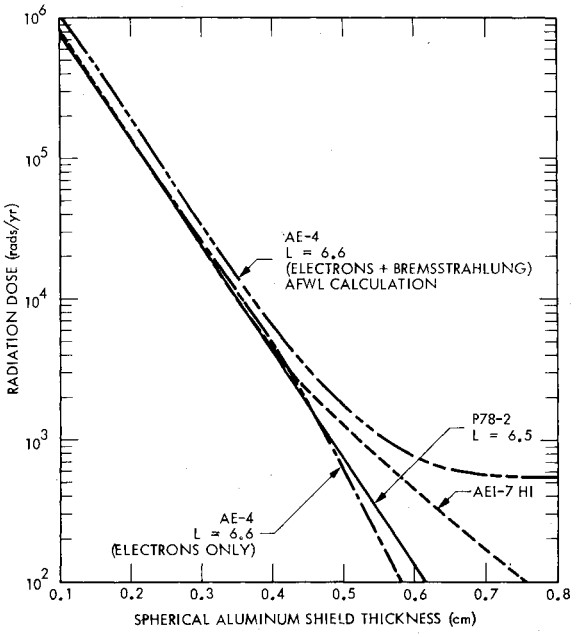

Fig. 6 Yearly radiation dose acquired as a function of spherical aluminum shielding thickness in the geosynchronous orbit using the AE-4, AEI-7 HI and P78-2 electron spectra.

the bremsstrahlung created in the stopping of the electrons in the shield is not determined in the AURORA program.

The yearly electron dose (rad/yr) acquired by a geosynchronous satellite for the AE-4, AEI-7 HI, and the P78-2 spectra using this program are shown in Fig. 6 as a function of shield thickness up to 0.8 cm. For orientation to the reader, a typical electronic component in an enclosure located behind a satellite skin will have an inherent shielding of ~0.25 cm. Also shown in Fig. 6 is a calculation of the yearly dose acquired with the AE-4 spectra using a Monte Carlo approach and also including the contributions of the bremsstrahlung (Janni[13]). The differences in the curves at the small shield thicknesses reflect the accuracies obtainable with the two independent approaches. The results from the AE-4, AEI-7, and P78-2 spectra as calculated with the AURORA program are identical up to shield thicknesses of ~0.45 cm at which thickness the dose level is 2000 rad. For thicker shields, i.e. for those cases where sensitive components are involved that cannot survive 2000 rad for a one-year mission or for longer mission considerations, the divergent impact of the AEI-7, P78-2, and AE-4 spectra become apparent. Behind 0.55 cm shield thickness the yearly dose resulting from the P78-2 and AEI-7 spectra are a factor of 1.5 and 3.6 higher, respectively, than that produced by the AE-4 spectrum. The AEI-7 LO model can be considered conservative for dose determinations while the AE-4 and AEI-7 HI models underestimate and overestimate, respectively, the actual dose received. Establishing the validity of the P78-2 electron fluence for long-term dose predictions must, however, await the analysis of a larger final-orbit data base. These differences would be significant were it not for the fact that at these shield thicknesses the bremsstrahlung contribution begins to dominate the total dose as evidenced by the flattening of the curve in the AFWL calculations. Thus, from a practical point of view the total dose acquired behind very thick shields is relatively independent of the electron model used and is determined predominantly by the bremsstrahlung created by the more intense electrons at the lower energies where the various models are in agreement.

Conclusions

The energetic electron spectra measured during the three-day period of the P78-2 transfer orbit are in better agreement with the AE-4 radiation model than the AEI-7 HI or LO models, although the former does not properly account for the measured flux >4 MeV. These data are representative of a magnetically quiet period some 10 days after a moderate storm occurred in the magnetosphere. Analysis of a larger data base from the SC-3 instrument in the P78-2 final orbit, including both storm and quiet periods, is required before the relevance of the present measurements to long term temporal averages can be established. It is shown that the total radiation does acquired behind thin shields (<0.45 cm aluminum) in the geosynchronous orbit is relatively independent of the model used. Behind thick shields the dose is dominated by the bremsstrahlung created by the lower energy electrons in a range where the various modes are in agreement. The model differences in spectral shape at the higher energies are therefore not highly significant in terms of the radiation dose accumulated.

Acknowledgments

The SC-3 experiment on the P78-2 spacecraft is sponsored by the Office of Naval Research under Contract N00014-76-C-0444. Partial support for analysis of the satellite data have also been provided by the USAF-Space Division through the Office of Naval Research and by the Lockheed Independent Research program. The use of the computer facilities at the National Space Science Data Center to generate the *B,L* data for the transfer orbit is greatly appreciated.

References

[1] Stevens, J.R. and Vampola, A.L., "Description of the Space Test Program P78-2 Spacecraft and Payloads," SAMSO TR-78-24, Sec. 9, Oct. 31, 1978, p. 29.

[2] Vampola, A.L., Blake, J.B., and Paulikas, G.A., "A New Study of the Outer Zone Electron Environment: A Hazard to CMOS," AIAA Paper 77-40, AIAA 15th Aerospace Sciences Meeting, Los Angeles, Calif., Jan. 1977.

[3] Berger, M.J., Seltzer, S.M., Chappell, S.E., Humphreys, J.C., and Motz, J.W., "Table of Response Functions for Silicon Electron Detectors," National Bureau of Standards Technical Note 489, Aug. 1969.

[4] Barraclough, D.R., Harwood, J.M., Leaton, B.R., and Malin, S.R.C., "A Model of the Geomagnetic Field at Epoch 1975," *Geophysical Journal of the Royal Astronomical Society,* Vol. 43, 1975, pp. 645-659.

[5] Olson, W.P., Pfitzer, K.A., and Mroz, G.J., "Modeling the Magnetospheric Magnetic Field," *Quantitative Modeling of Magnetospheric Processes,* edited by W.P. Olson, American Geophysical Union, Washington, D.C., 1979, pp. 77-85.

[6] McIlwain, C.E., "Coordinates for Mapping the Distribution of Magnetically Trapped Particles," *Journal of Geophysical Research,* Vol. 66, 1961, p. 3681-3691.

[7] Singley, G.W., and Vette, J.I., "A Model Environment for Outer Zone Electrons," National Space Science Data Center Report 72-13, Dec. 1972.

[8] Chan, K.W., Teague, M.J., Schofield, N.J., and Vette, J.I., "Modeling of Electron Time Variations in the Radiation Belts," *Quantitative Modeling of Magnetospheric Processes,* edited by W.P. Olson, American Geophysical Union, Washington, D.C., 1979, pp. 121-149.

[9] West, H.I., Jr., Buck, R.M., and Dividson, G., "Study of Energetic Electrons in the Outer Radiation-Belt Regions Using Data Obtained by the LLL Spectrometer on OGO-5 in 1968," University of California Research Laboratory Report 52807, July 26, 1979.

[10] Vampola, A.L., Blake, J.B., and Paulikas, G.A., "A New Study of the Magnetospheric Electron Environment," *Journal of Spacecraft and Rockets,* Vol. 14, 1977, pp. 690-695.

[11] Kennel, C.F., and Petschek, H.E., "Limit of Stably Trapped Particle Fluxes," *Journal of Geophysical Research,* Vol. 71, 1966, p. 1.

[12] Walt, M., McDonald, W.M., and Francis, W.E., "Penetration of Auroral Electrons into the Atmosphere," *Physics of the Magnetosphere,* edited by R. Carovillano and J.G. McClay, Reinhold, New York, 1968, pp. 534-555.

[13] Janni, J., private communication, USAF Weapons Laboratory, Albuquerque, N. Mex., 1976.